Supporting Information

Influence of support on the rhodium speciation and catalytic activity of rhodium-based catalysts for total oxidation of methane

Yu Zhang[1], Peter Glarborg[1], Martin Peter Andersson[1], Keld Johansen[2], Thomas Klint Torp[2], Anker Degn Jensen[1], Jakob Munkholt Christensen[1]*

[1]Department of Chemical and Biochemical Engineering, Technical University of Denmark (DTU), Søltofts Plads 229, 2800 Kgs. Lyngby, Denmark.

[2]Haldor Topsoe A/S, Haldor Topsøes Allé 1, 2800 Kgs. Lyngby, Denmark

*email: jmc@kt.dtu.dk

S1. XRD of Rh/ZSM-5(30)-IE and the pure support.

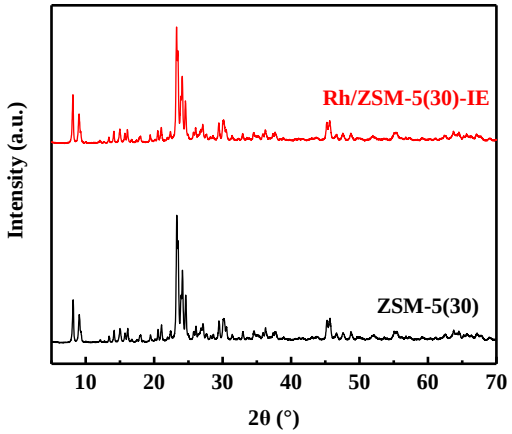

Fig. S1. XRD pattern of ZSM-5(30) zeolite and Rh/ZSM-5(30)-IE catalyst.

Fig. S1 confirmed the MFI structure of ZSM-5(30) zeolite. The XRD pattern of the ion exchanged Rh/ZSM-5(30)-IE looks identical to the one for the pure support, indicating that no Rh nanoparticles were formed on this sample and this is in good agreement with electron microscopy (Fig. 4 (b) in the main text) and CO-DRIFTS (Fig. 5 in the main text).

S2. Activity of Rh based catalysts for CH_4 oxidation

2.1 CH_4 oxidation on Rh/ZSM-5(30)-IE

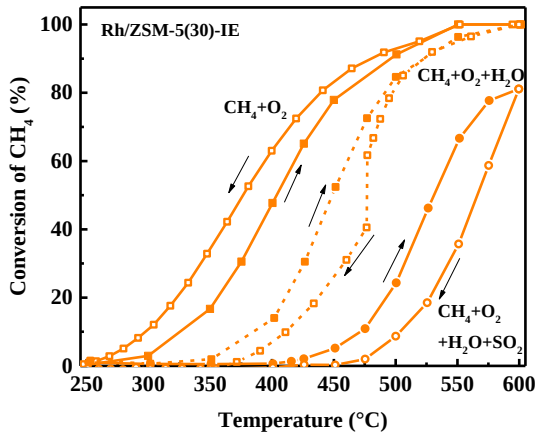

Fig. S2. Conversion of CH_4 over Rh/ZSM-5(30)-IE in different reaction atmospheres. Rea-1:CH_4+O_2, Rea-2:CH_4+O_2+H_2O, and Rea-3: CH_4+O_2+H_2O+SO_2. Test conditions: 2500 ppm CH_4, 10 vol% O_2, 5 vol% H_2O when present, 20 ppm SO_2 when present, balanced with N_2, GHSV=150,000 N ml g_{cat}^{-1} h^{-1}.

Fig. S2 shows the CH_4 conversion with the ion-exchanged catalyst in various gas atmospheres. After running in CH_4+O_2 reaction gas in the 1st run an activation phenomenon was seen from the higher CH_4 conversion in the 2nd run. This suggests the generation of a more active phase during CH_4 oxidation. The activation effect however, is only visible below 475 °C. As characterization of the spent catalyst (Fig. 8 in the main text and Fig. S6) shows that small nanoparticles have emerged during the test, the activation is attributed to a higher intrinsic activity of Rh_2O_3 nanoparticles compared to Rh single atom sites. Water added to the feed caused severe deactivation to the single Rh site containing catalyst, which is seen from both a lower activity than in dry conditions, a significantly lower activity in the 2nd run, and in a continuous activity drop at 475 °C in 15 h (Fig. S4). Strong deactivation also occurred in the combined presence of water and SO_2. The significant inhibition by both water and SO_2 is a characteristic feature of the Al rich zeolites, with a large fraction of the Rh as single atom sites.

2.2 CH_4 oxidation on 2 wt% Rh catalysts

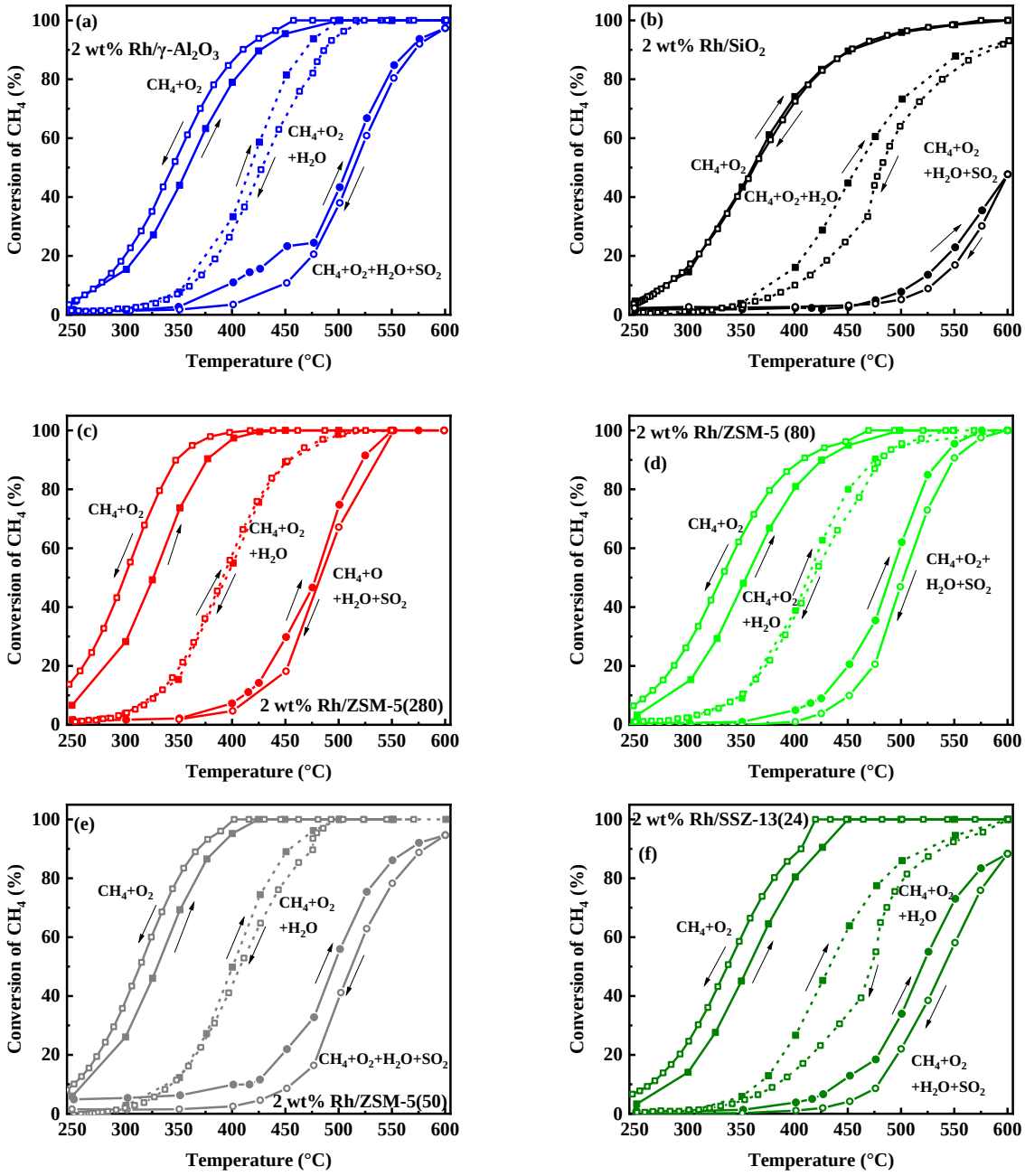

Fig. S3. Conversion of CH_4 over 2 wt% Rh catalysts in different reaction atmospheres. Rea-1: CH_4+O_2, Rea-2: $CH_4+O_2+H_2O$, and Rea-3: $CH_4+O_2+H_2O+SO_2$. (a): 2 wt% Rh/γ-Al_2O_3; (b): 2 wt% Rh/SiO_2; (c): 2 wt% Rh/ZSM-5(280); (d): 2 wt% Rh/ZSM-5(80); (e): 2 wt% Rh/ZSM-5(50); (f): 2 wt% Rh/SSZ-13(24). Test conditions: 2500 ppm CH_4, 10 vol% O_2, 5 vol% H_2O when present, 20 ppm SO_2 when present, balanced with N_2, GHSV=150,000 N ml g_{cat}^{-1} h^{-1}. Figure includes 2 wt% Rh/ZSM-5(280) data from Zhang et al. [1].

All the Rh catalysts experienced an activation process in the 1st run in the pure CH_4+O_2 (Rea-1) reaction gas and exhibit higher conversion in the 2nd run except for 2 wt% Rh/SiO_2, although the effect is smaller than for the ion-exchanged sample in Fig. S2. With addition of 5 vol% H_2O to the feed (Rea-2), all the catalysts suffered from inhibition by H_2O and showed lower activity compared with the dry conditions. The activity in the 2nd run was also lower than the one in the 1st run, and the difference between the two runs is more significant for the Al rich zeolite supported catalysts. Smallest difference between the two subsequent runs in the presence of H_2O was observed on the Si rich zeolite, ZSM-5(280), supported catalyst. More proton and Al rich zeolites are thus more susceptible to water inhibition. With further addition of 20 ppm SO_2, a further deactivation occurred and lower CH_4 conversion was achieved. 2 wt% Rh/ZSM-5(280) is the most active and stable catalyst in both H_2O and SO_2 containing reaction gas. The deactivation in the subsequent two runs can be correlated to the Al content in the zeolite with higher Al content leading to larger deactivation, which is the same as the trend in the only H_2O containing atmosphere.

2.3 Stability of Rh based catalysts in the presence 5 vol% H_2O at 475 °C.

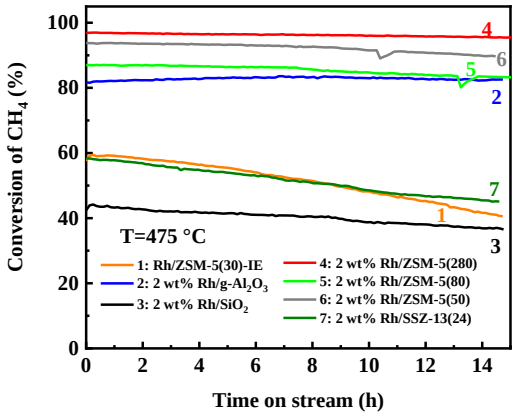

Fig. S4. Stability of Rh based catalysts: 1: Rh/ZSM-5(30)-IE(orange), 2: 2 wt% Rh/g-Al_2O_3 (blue), 3: 2 wt% Rh/SiO_2 (black), 4: 2 wt% Rh/ZSM-5(280) (red), 5: 2 wt% Rh/ZSM-5(80) (green), 6: 2 wt% Rh/ZSM-5(50) (gray), 7: 2 wt% Rh/SSZ-13(24) (olive) at 475 °C in 5 vol% H_2O containing atmosphere. Test conditions: 2500 ppm CH_4, 10 vol% O_2, 5 vol% H_2O, in N_2, GHSV=150,000 N ml g_{cat}^{-1} h^{-1}. Figure includes 2 wt% Rh/ZSM-5(280) data from Zhang et al. [1].

The 2 wt% Rh/SiO_2 catalyst, the single Rh atom rich catalysts, Rh/ZSM-5(30)-IE and 2 wt% Rh/SSZ-13(24) all deactivated significantly during the 15 h stability test at 475 °C in the presence of 5 vol% H_2O. The catalyst with the Si-rich zeolite support, Rh/ZSM-5(280), was active and stable in the H_2O containing reaction gas showing the superior stability of Si-rich zeolites.

2.4 Stability at 450 and 500 °C in the presence of 5 vol% H_2O and 20 ppm SO_2.

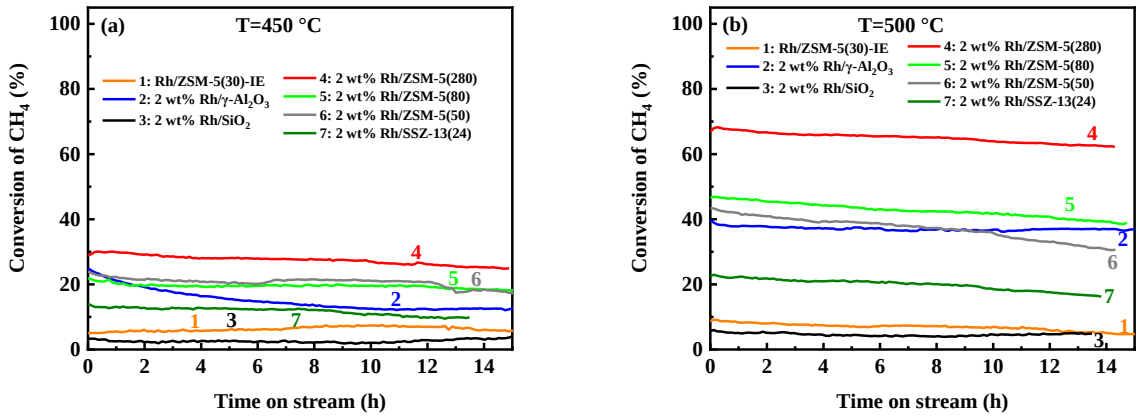

Fig. S5. Stability of Rh based catalysts for CH_4 oxidation in the presence of 5 vol% H_2O and 20 ppm SO_2 at (a): 450 °C in the 1st run during heating and (b): 500 °C in the 2nd run during cooling. 1: Rh/ZSM-5(30)-IE(orange), 2: 2 wt% Rh/g-Al_2O_3 (blue), 3: 2 wt% Rh/SiO_2 (black), 4: 2 wt% Rh/ZSM-5(280) (red), 5: 2 wt% Rh/ZSM-5(80) (green), 6: 2 wt% Rh/ZSM-5(50) (gray), 7: 2 wt% Rh/SSZ-13(24) (olive). Test conditions: 2500 ppm CH_4, 10 vol% O_2, 5 vol% H_2O, balanced with N_2, GHSV=150,000 N ml g_{cat}^{-1} h^{-1}. Figure includes 2 wt% Rh/ZSM-5(280) data from Zhang et al. [1].

2 wt% Rh/ZSM-5(280) which is rich in Rh nanoparticle sites is the best performing Rh catalyst in the H_2O and SO_2 containing reaction gas in terms of CH_4 conversion and the stability during time on stream test. Generally the catalysts are relatively stable in the presence of SO_2 (once the uptake by the support has saturated).

S3. Characterization of spent catalysts

3.1 HAADF-STEM-EDS analysis of spent Rh/ZSM-5(30)-IE

3.1.1 After CH_4+O_2

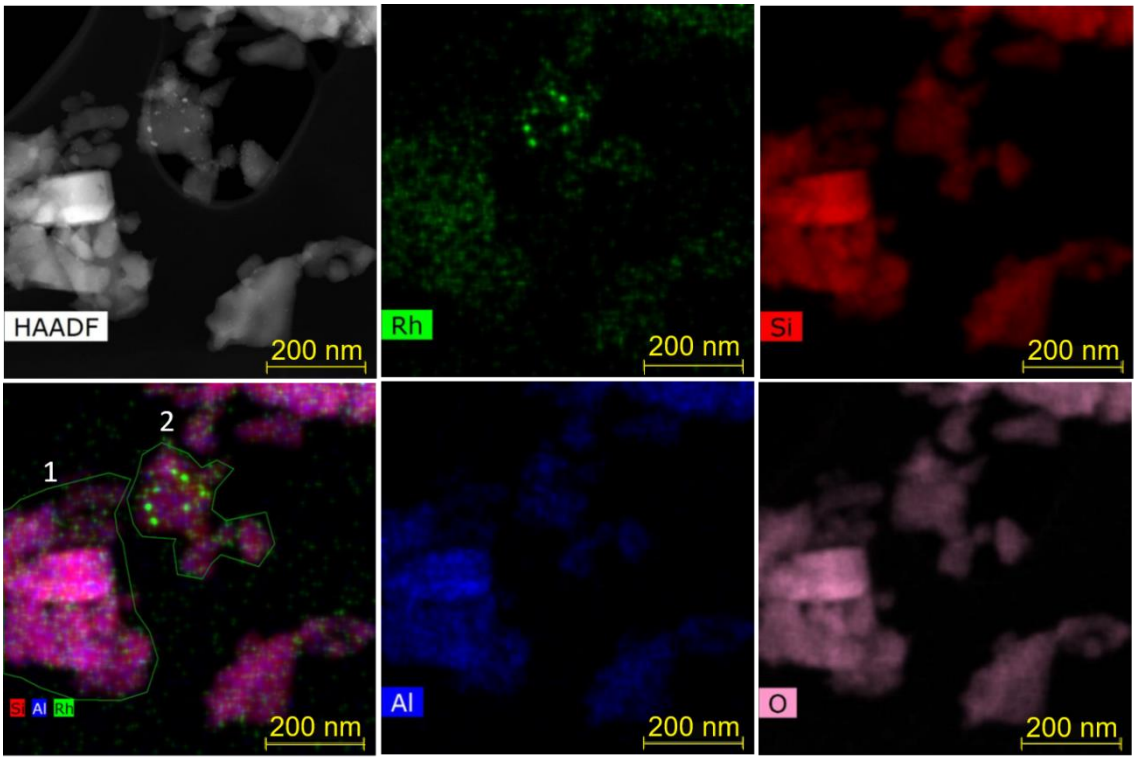

Fig. S6. HAADF-STEM-EDS analysis of Rh/ZSM-5(30)-IE catalyst after running in 2500 ppm CH_4 + 10 vol% O_2. The STEM picture and EDS analysis of the fresh catalyst in shown in Fig. 3 (b) and Fig. 4 (b) in the main text.

Compared to the very homogeneous atomic dispersion of Rh in the fresh state of the ion-exchanged catalyst in Fig. 4 (b) in the main text the Rh distribution of the spent Rh/ZSM-5(30)-IE became more inhomogeneous as shown in Fig. S6. The determined Rh loading in the area labeled by 1 and 2 are 0.45±0.23 wt% and 1.51±0.60 wt% respectively. The Rh loading in the fresh catalyst is 0.44±0.21 wt% by EDS and 0.294 ± 0.015 wt% determined by ICP-OES method as mentioned in section 1.3 in the main text. The inhomogeneity and presence of Rh rich zones indicate the formation of Rh nanoparticles after CH_4 oxidation reaction.

3.1.2 After $CH_4+O_2+H_2O$

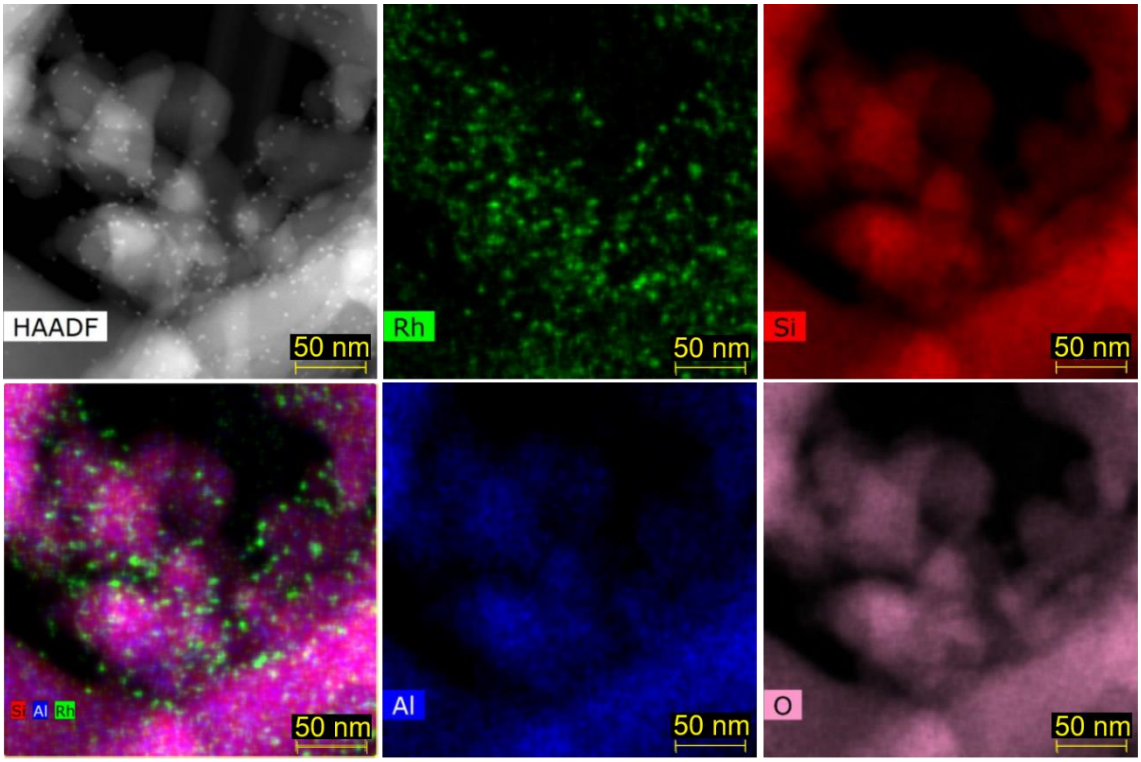

Fig. S7. HAADF-STEM-EDS analysis of Rh/ZSM-5(30)-IE catalyst after running in 2500 ppm CH_4 + 10 vol% O_2 + 5 vol% H_2O. The STEM picture and EDS analysis of the fresh catalyst in shown in Fig. 3 (b) and Fig. 4 (b) in the main text.

Reaction in $CH_4+O_2+H_2O$ also appears to lead to agglomeration of the single atom sites into nanoparticles. The Rh loading in the analyzed area of the spent catalyst after CH_4 oxidation in $CH_4+O_2+H_2O$ atmosphere (Fig. S7) was determined to be 0.67 ±0.28 wt% and the deviation from the bulk content (0.294 wt%) suggests an increasing inhomogeneity. The presence of Rh nanoparticles outside the zeolite structure was confirmed by the EDS analysis.

S4 References for the supporting information

1 Y. Zhang, P. Glarborg, K. Johansen, M. P. Andersson, T. K. Torp, A. D. Jensen and J. M. Christensen, *ACS Catal.*, 2020, **10**, 1821–1827.